Engineering Structures 48 (2013) 43–54

Contents lists available at SciVerse ScienceDirect

Engineering Structures

journal homepage: www.elsevier.com/locate/engstruct

Effect of steel wrapping jackets on the bond strength of concrete and the lateral performance of circular RC columns

Eunsoo Choi [a,1], Young-Soo Chung [b,2], Kyoungsoo Park [c], Jong-Su Jeon [d,*]

[a] Department of Civil Engineering, Hongik University, Seoul 121-791, Republic of Korea
[b] Department of Civil Engineering, Chung-Ang University, Seoul 156-756, Republic of Korea
[c] School of Civil and Environmental Engineering, Yonsei University, Seoul 120-749, Republic of Korea
[d] School of Civil and Environmental Engineering, Georgia Institute of Technology, Atlanta, GA 30332, USA

ARTICLE INFO

Article history:
Received 28 January 2012
Revised 17 August 2012
Accepted 27 August 2012
Available online 21 November 2012

Keywords:
Steel wrapping jacket
Seismic retrofit
Bond strength
Lap splice slippage
Buckling fracture of reinforcement

ABSTRACT

In this study, the bond behavior between steel reinforcing bars and concrete confined via steel wrapping jackets is estimated. Lateral bending tests are conducted for the reinforced concrete columns with continuous longitudinal reinforcement or lap-spliced longitudinal bars confined by the steel wrapping jackets. It is found that the jackets increase the bond strength and ductile behavior due to the transfer of splitting bonding failure to pull-out bonding failure. In the column tests, the steel wrapping jackets increase the flexural strength and ultimate drift for the lap-spliced column. However, the jacket for the column with continuous longitudinal reinforcement only increases the ultimate drift since the flexural strength depends on the yield of reinforcement. Finally, this study suggests a basic concept for determination of the thickness of the steel wrapping jackets which is different from the conventional method.

1. Introduction

With the prevalence of social media and the Internet since the late 1990s, the knowledge of major seismic events in more heavily populated areas, such as Chirstchurch in New Zealand and Tohoku in Japan, has increased and thus, the public perception of "safe" structures is becoming more important. Therefore, it is sensible to emphasize seismic protection for civil structures with a particular goal of placating public perception of the safety of the civil structures. Most countries in area of high or moderate seismic risk have seismic codes that reflect their seismic situations and design philosophies. However, bridges that have been in service for long periods of time may not have sufficient seismic protection due to their non-seismic design and construction. Bridge failures during previous earthquakes have been primarily caused by inadequate construction details such as inadequate lateral reinforcement or insufficient lap length of the bars [1–4]. Sometimes, even structures that have been constructed according to seismic codes require seismic retrofitting when the seismic hazard in the area is re-estimated and the risk level is estimated to have increased [5]. Accordingly, many of bridges are exposed to seismic hazards and require seismic retrofit plans. For reinforced concrete (RC) columns, external jackets have been proven to be effective in providing seismic protection and increasing the ductile behavior of the columns [6,7]. Steel and fiber reinforced polymer (FRP) jacketing methods have been proposed and have demonstrated good performance for the seismic protection of RC columns [8–10]. However, these two methods possess critical drawbacks such as grouting for steel jackets or bonding for FRP jackets. The grouting of the steel jackets increases the cross-sectional area and creates the discontinuity in the column surface. Also, the grouting bonds the steel jacket to the concrete surface, and the steel jacket enhances the flexural stiffness and shortens the fundamental natural period of the column as indicated by Bracci et al. [11]. This may have a negative effect on the column because the shortened natural period draws more seismic inertia force. The bonding of the FRP jackets with an adhesive such as epoxy causes a problem of wrinkles in the FRP sheet surface. These wrinkles inhibit the confining action on the concrete and reduce the effectiveness of the FRP jacket. Researchers have attempted to introduce prestress on the FRP sheet in order to solve this problem; however, a large device is required to accomplish this [12].

For retrofit of RC beam–column joints, Karayannis et al. [13] proposed the use of a thin and locally applied steel jacket to eliminate the disadvantages of cast-in-place concrete or shotcrete jacketing techniques requiring labor-intensive procedures [14]. For

* Corresponding author. Tel.: +1 404 895 5241; fax: +1 404 894 1641.
E-mail addresses: eunsoochoi@hongik.ac.kr (E. Choi), chung47@cau.ac.kr (Y.-S. Chung), k-park@yonsei.ac.kr (K. Park), jongsu.jeon@gatech.edu (J.-S. Jeon).
[1] Tel.: +82 2 320 3060; fax: +82 2 322 1244.
[2] Tel.: +82 2 820 5054.

0141-0296/$ - see front matter © 2012 Elsevier Ltd. All rights reserved.
http://dx.doi.org/10.1016/j.engstruct.2012.08.026

Nomenclature

A_{bl}	area of one main column reinforcing bar	H	height of the column
A_g	gross area of the column cross-section	L	length of the column
c	thickness of the concrete cover for the longitudinal steel bars	L_b	development length
D	diameter of the column	L_s	length of the lap splice
d_b	nominal bar diameter	l_j	length of the steel jackets
d_{lb}	diameter of a longitudinal bar	n	number of spliced bars along p
E_j	elastic modulus of the jacket	P	tension of the cable
E_t	elastic modulus in tension	p	perimeter in the column cross section along the lap-spliced bar locations
F	applied force in the bar	ρ_l	volumetric ratio of longitudinal reinforcing bar
f'_c	peak compressive strength of the unconfined concrete	$s_{\max}$	slip limit for the ultimate bond stress
f_{ck}	specific concrete strength	s_2	limit for the stable bond stress range
f_h	confining pressure provided by the transverse steel reinforcement at the strain level of 0.1%, $f_{je} = 1.1f_{yj}$	s_f	slip starting frictional slippage
		t_j	required thickness of the steel jacket
f_l	required lateral clamping pressure	τ_b	bond stress of a reinforcing bar
f_s	stress at the bar	$\tau_{b,\max}$	maximum bond strength
f_{yj}	yield strength of the steel plate	$\tau_{b,f}$	frictional bond strength
f_{yl}	yield strength of longitudinal bars	W	width of the jacket

monolithical beam–column joints, the application of steel jackets changed a joint shear failure to a ductile flexural failure [15]. However, the study of Engindeniz et al. [16] indicated that the use of the steel jackets for beam–column joints has disadvantages such as potential for corrosion, difficulty in handling and in application for actual three-dimensional joints. Recently, a new jacketing method using shape memory alloy wires was proposed in an effort to overcome the problems of grouting and adhesives, and its effectiveness was proved through experimental tests [17–19]. However, several researchers have noted the price of shape memory alloys as a critical obstacle to their use in seismic retrofitting [20,21]. Steel is the cheapest material among these three materials, and steel jackets are very effective to improve ductile behavior for seismically deficient RC columns [22–24]. Choi et al. [25] suggested a steel wrapping jacket without grouting and demonstrated the effectiveness of the jacketing method through axial compressive tests of concrete cylinders. The steel wrapping jackets increased the peak strength and ductility of the concrete by providing external confinement. However, the bonding behavior of the concrete confined by the steel wrapping jacket has not yet been discussed.

The bond between the steel reinforcing bars and concrete is a crucial factor for RC columns exposed to seismic events. In particular, RC columns with lap-spliced reinforcements in the plastic region demonstrated a splitting bond failure and did not provide adequate ductility [26]. Pull-out failures develop under conditions of sufficiently thick concrete cover or well confinement. The pull-out mode demonstrated higher bond strength and more toughness than the splitting mode. Therefore, the external confinement can transform the splitting mode into the pull-out mode by providing additional external confinement. Pull-out tests for the steel-encased specimens subjected to reverse cyclic loading have been conducted [27], and the specimens in the study were fabricated using a preparation of a steel tube inside which the concrete was poured. For this case, the composite behavior was developed between the steel and the concrete, and this simulated the grouted steel jackets.

The first aim of this study is to demonstrate that steel wrapping jackets increase the bond strength of concrete. While steel wrapping jackets have been applied previously to confine lap-spliced RC columns, the results were not satisfactory [28]. The previous study was a partially successful test because their specimens experienced degrading behavior after reaching the yield. Therefore, the second aim of this study is to propose a new wrapping method for the steel wrapping jackets in order to demonstrate force–displacement behavior without degradation and to explain how steel wrapping jackets affect the failure mode of RC columns.

2. Bonding behavior of concrete confined by steel wrapping jackets

2.1. Specimens and test setup

In this study, the specimens of concrete cylinders prepared were expected to induce splitting bond failure in an unconfined state; concrete cylinders with dimensions of 100 mm × 200 mm were used. Stainless steel jackets with the dimensions of 324 mm × 200 mm were prepared in order to confine the concrete cylinders; the width was 10 mm larger than the perimeter of the cylinder in order to create the welding overlap. Steel jacket thicknesses of 1.0 mm and 1.5 mm were chosen to assess how the amount of confinement has an effect on the bond behavior. There were three types of specimens for the splitting failure mode: (1) unconfined, (2) confined by a 1 mm jacket, and (3) confined by a 1.5 mm jacket. Each type had two specimens, and a total of six specimens were prepared for the bonding tests.

The yield strength of the steel jackets was measured to be 288 MPa, and the measured peak strength of the concrete was 30 MPa. The total length of the reinforcing bars was 260 mm, and a part measuring 60 mm protruded beyond the top surface of the specimens. The embedment length of the bars was 150 mm, with 25 mm of length at the top and bottom of the specimens wrapped with oil paper. The D22 reinforcing bar (with a nominal diameter of 22.2 mm) was used in the tests. The detail description of the jacketing process can be found in Choi et al. [25]. Fig. 1 shows the jacketing process briefly. First, a rolled steel jacket was prepared and the concrete surface was treated. Then, two clamps and three steel bands were used to press the steel jacket onto the concrete surface. Next, the steel jacket under an external pressure was welded and attached tightly to the concrete surface after the subsequent removal of the clamps and the steel bands.

The bond test in this study was a push-out test, and Fig. 2 illustrates the test setup graphically. A specimen was placed on a support frame that has a circular rigid plate at the top with a hole of 25 mm at the center of the plate. The protruding reinforcing bar

(a) Bended steel jacket (b) Surface treatment

(c) Clamping steel jacket (d) Welding steel jacket

(e) Completed specimen

Fig. 1. Process for steel wrapping jackets.

was pushed down through the hole by an actuator, and the slip was measured by a displacement transducer fixed using a magnetic base on the bottom plate of the support frame. The measured slip of the reinforcing bar was used to calculate the bond stress. During the push-out process, the compression plate in Fig. 2b was just contacted on the top of the extrusion bar and thus, the connection was similar to a pin and any bending loading was not transferred to the bar. All specimens were pushed out up to 22 mm, which is the distance from the start of one rib to the end of an adjacent rib of the reinforcement.

2.2. Bond test results

The failure mode of the unconfined specimens was the splitting mode as initially planned. Figs. 3 and 4 indicate the inside and outside views of the unconfined and confined specimens after the

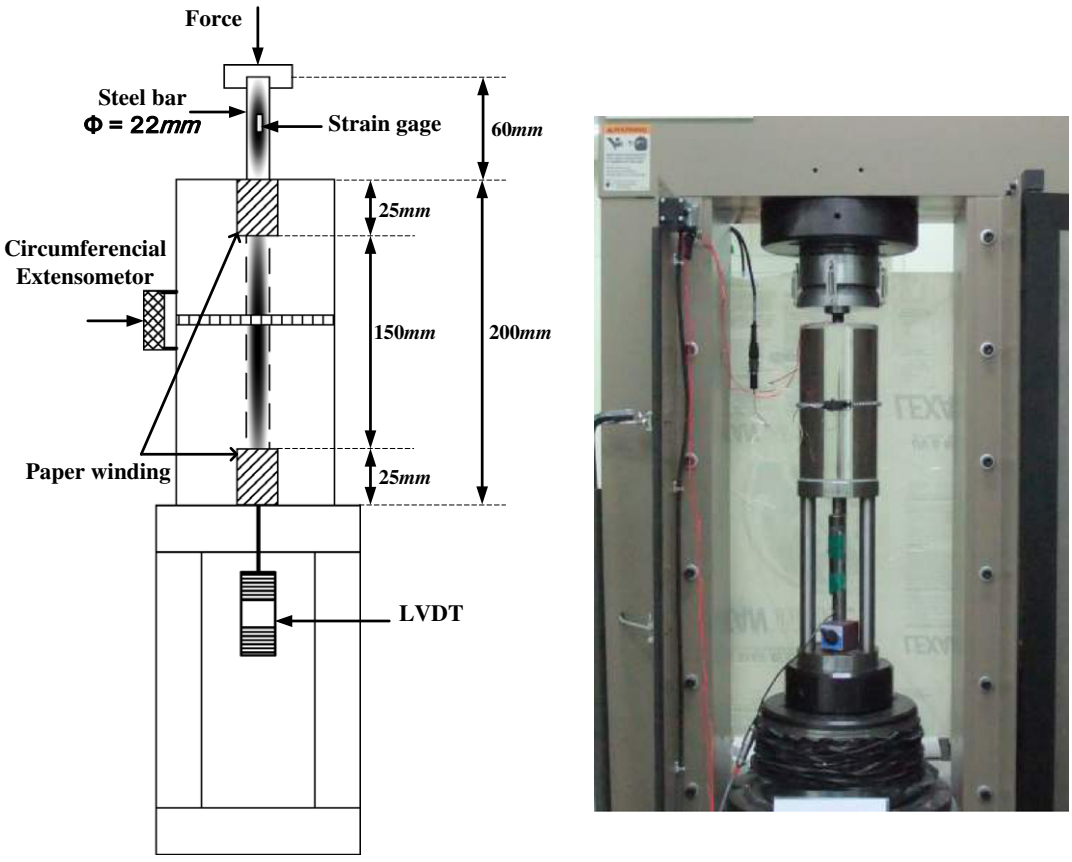

(a) Specimen-dimensions and instruments (b) Picture of test set-up

Fig. 2. Schematic of test setup.

(a) Side view (b) Top view (c) Inside view

Fig. 3. Splitting failure mode of unconfined concrete.

completion of the test, respectively. For the splitting failure mode, radial cracks developed due to the splitting stress, and the concrete surface contacting the reinforcing bar was clear because the bar slipped on the surface. For the pull-out failure mode, the radial crack was not visible to the naked eye. The concrete between the ribs of the reinforcing bar was sheared off, and the smoothened contact surface was attributed to the friction between the two concrete surfaces.

Assuming that the bond stress (τ_b) of a reinforcing bar embedded in the concrete is distributed uniformly over the development length (L_b), the applied force (F) in the bar can be calculated from the equilibrium of forces as follows:

$$F = \tau_b \pi d_b L_b \tag{1}$$

where d_b is the nominal bar diameter of 22.2 mm and the uniform bond stress for each specimen was calculated using Eq. (1). The experimental bond stress–slip curves were compared with the nonlinear expression provided by Ciampi et al. [29] to check the accuracy of the experimental results. The above bond stress–slip model does not concern uncracked concrete essentially. As a

(a) Side view (b) Top view (c) Inside view

Fig. 4. Pull-out failure mode of concrete confined using a steel wrapping jacket.

consequence, it provides general validity for nonlinear empirical expression of bond stress–slip relationship. The analytical model was divided into four parts: (1) the initial loading phase in Eq. (2), (2) the plateau state, (3) the linear softening phase, and (4) the residual stable plateau. Each state is described below:

$$\tau_b = \tau_{b,\max}\left(\frac{s}{s_{\max}}\right)^{\alpha} \quad 0 \leqslant s \leqslant s_{\max} \tag{2}$$

The pull-out bond failure: $s_{\max} = 1$ mm, $s_2 = 3$ mm, $s_f =$ clear rib spacing

$$\tau_{b,\max} = 2.5f_{ck}^{1/2} \quad \tau_{b,f} = f_{ck}^{1/2}, \text{and } \alpha = 0.4$$

The splitting bond failure: $s_{\max} = s_2 = 0.6$ mm, $s_f = 1$ mm

$$\tau_{b,\max} = 2.0f_{ck}^{1/2} \quad \tau_{b,f} = 0.3f_{ck}^{1/2}, \text{ and } \alpha = 0.4$$

where $\tau_{b,\max}$ and $\tau_{b,f}$ represent the maximum bond strength and the frictional bond strength value, respectively. Also, the $s_{\max}$ is the slip limit for the maximum bond stress, s_2 is the limit for the stable bond stress range, and s_f is the slip starting frictional slippage. Table 1 shows the bonding strengths of the unconfined and confined specimens. In addition, Fig. 5 shows the bond stress–slip relationship and the comparison between the experimental results and analytical model. The results of the unconfined and confined specimens are compared in Fig. 5d. As indicated in Fig. 5a, the experimental results for the splitting failure mode correspond well to the analytical model. However, in the case of the pull-out failure mode for the confined specimens in Fig. 5b and c, the experimental curves did not show a plateau phase following an increasing branch as the model does, although the other sections matched with the model well. The bond stress–slip curves in previous studies did not demonstrate the plateau for the pull-out failure mode clearly [27,30]. The steel jackets demonstrated an increment of bond strength of 65.3% for a 1.0 mm jacket and 73.5% for a 1.5 mm jacket. The 1.5 mm jackets increased the bond strength by 5.0% on average compared to the 1.0 mm jacket. It appears that a critical confinement exists beyond which the bond strength does not increase confinement. The investigation of the experimental results demonstrated that the steel wrapping jackets increased the bond strength of the reinforced concrete although it did not provide the composite behavior between the steel jacket and the concrete in the axial direction.

Table 1
Bonding strengths of specimens.

Specimen	Unconfined (MPa)	Steel-1.0 mm (MPa)	Steel-1.5 mm (MPa)
SP-1	9.50	17.23	17.70
SP-2	10.84	16.39	17.60
Average	10.17	16.81	17.65

3. Test preparation of the RC columns confined by steel wrapping jackets

3.1. Specimen preparation

Four circular columns, each 400 mm in diameter and 1400 mm in height, were fabricated with a ratio of 3.5, as indicated in Fig. 6. Each column was fabricated with 16-D13 longitudinal bars and D10 bars with a spacing of 160 mm for the transverse reinforcement. The concrete cover of the specimens was 40 mm. The measured yield strength of the longitudinal reinforcements was 325 MPa, and the measured compressive strength of the concrete was 20 MPa.

Two of the four columns had a 50% lap splice in the longitudinal reinforcements from the starter bars projecting from the foundation. These specimens are indicated as SP50-NSJ and SP50-SJ1 in Table 2. In this paper, NSJ refers to the non-steel jacket and SJ1 represents the specimen with steel jackets. A 50% lap splice indicates that half of the 16 bars were spliced from the starter bars, and the length of a lap splice was 200 mm. The remaining columns were constructed with continuous longitudinal reinforcements and are indicated as SP00-NSJ and SP00-SJ1. One sample of each type of specimen was jacketed at the bottom of the column using the steel wrapping jacketing method. The steel jacket used to retrofit the bridge columns provides a lateral confining pressure on the concrete and can be considered as a continuous hoop reinforcement. The required thickness of the steel jacket (t_j) based on the equivalent volumetric ratio of the hoop reinforcement is generally calculated using the following three design equations

(a) ATC-32 [31]

$$t_j = \frac{D}{4}\left[\frac{0.16f_c'}{f_{je}}\left(0.5 + 1.25\frac{P}{f_c'A_g}\right) + 0.13(\rho_l - 0.01)\right] \tag{3}$$

where D is the column diameter; $f_{je} = 1.1f_{yj}$ in which f_{yj} is the yield strength of the steel plate; f_c' is the peak compressive strength of the unconfined concrete; A_g is the gross area of the column cross-section; and ρ_l is the volumetric ratio of longitudinal reinforcing bar.

(b) AASHTO [32]

$$t_j = 0.03D\frac{f_c'}{f_{yj}} \tag{4}$$

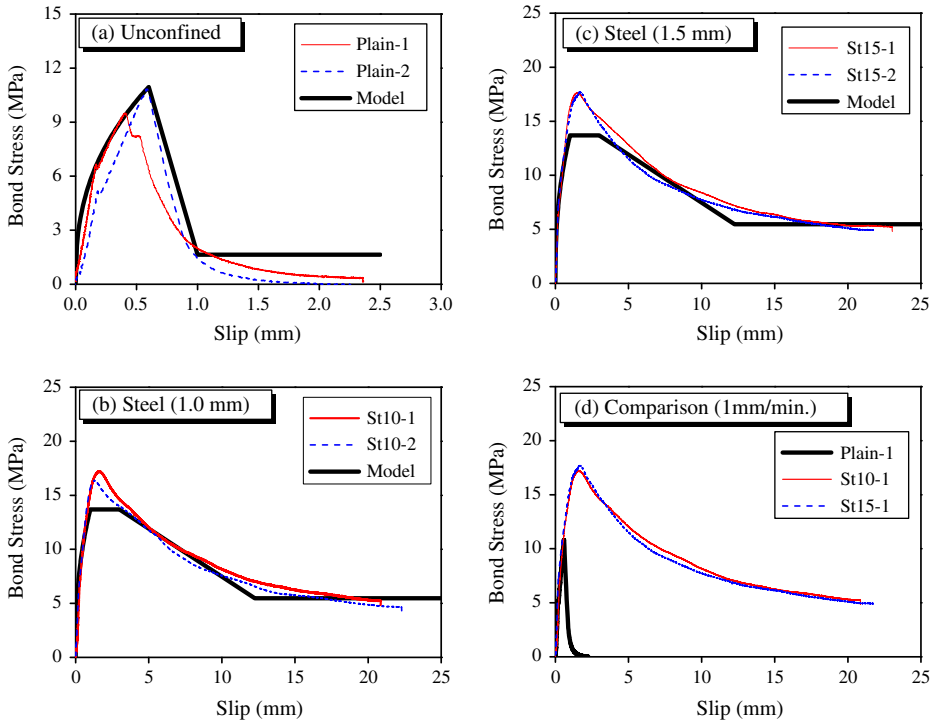

Fig. 5. Comparison of bond stress–slip relationship to an analytical model.

(c) Caltrans [33]

$$t_j = 0.03D\frac{f'_c}{f_{yj}}[0.5 + 1.25\frac{P}{f'_c A_g}] \quad (5)$$

The measured yield strength of the steel plate was 288 MPa. Using Eqs. (3)–(5), the estimated thicknesses of the steel jackets were 0.715 mm, 0.833 mm, and 0.521 mm for ACT-32, AASHTO, and Caltrans, respectively. The maximum thickness was 0.833 mm; therefore, this study used the 1.0 mm thickness for the steel plate conservatively. The length of the steel jackets (l_j) was determined to be 400 mm using the following equation [8]:

$$Max\left[\frac{l_j \geqslant D}{l_j \geqslant 0.25L}\right] \quad (6)$$

where D and L are the diameter and the length of the column, respectively.

The jacketing procedure for the columns was mechanically the same as that for the bonding test. However, clamps could not be used for the column; thus, the combination of a cable and a special device was used to press the steel jacket as shown in Fig. 7. The special device pulled the cable out by rolling a nut. A total of four cables were placed on the steel jacket, and the tension of the cable was estimated to be approximately 8.8 kN.

3.2. Test setup, instrumentation, and loading pattern

The test setup was established for a combination of axial and lateral loadings using the column footing assemblages, as shown in Fig. 8. A constant axial load of $0.1f'_cA_g$ was applied by introducing the prestressing force of two strands against the reinforced strong floor via a loading frame. Cyclic lateral loads were applied using a hydraulic actuator at a height of 1400 mm. All columns were instrumented to measure the lateral displacements and corresponding applied loads. The loads were measured using the calibrated load cell of the actuator. A displacement transducer was installed on the reference frame at a height of 1400 mm from the bottom of the footing. A quasi-static load was applied at the top of the columns under displacement control. A lateral load was applied in the form of a drift ratio starting from ±0.25%, which was first increased to ±0.5% and was then increased in 0.5% increments up to failure. Two cycles were applied for each drift ratio, which was the ratio of the input displacement to the column height of 1400 mm.

4. Test results of the RC columns confined by the steel wrapping jackets

4.1. Force–lateral displacement behavior

The cyclic behavior of the force–lateral displacement is shown in Fig. 9; the displacement was measured at the loading point using the actuator stroke. The corresponding envelope curves are illustrated in Fig. 10, and Table 3 presents the summary of the test results, such as the flexural strength, yield and ultimate drift ratios, and displacement ductility. The ultimate point was estimated to be 85% of the peak shear force in the degrading zone. The yield point was the intersection point of the horizontal line that indicates 85% of the peak force and the line from the origin to the point of 75% of the peak force. This study compared the average values of the pushing and pulling results. For the continuous reinforcement column SP00-NSJ, the yield and ultimate points occurred at a drift of 0.694% and 4.394%, respectively; the displacement ductility was 6.129. For the jacketed continuous reinforcement column SP00-SJ1, the yield and ultimate points were observed at 0.772% and 6.982%, respectively; thus, the displacement ductility was 9.059. The steel wrapping jacket increased the ultimate drift by 59.0% compared with that of the unjacketed specimen although the flexural strength of the jacketed specimen showed nearly the same strength as the unjacketed specimen. The flexural strengths for the two specimens were 97.1 and 94.6 kN, and the difference was only 2.6%. Accordingly, the steel jacket increased the ductile

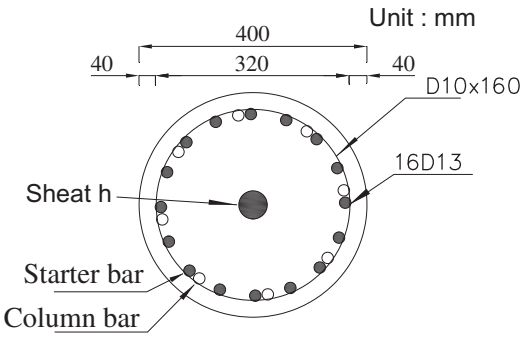

(a) Cross-section at lap-splice zone

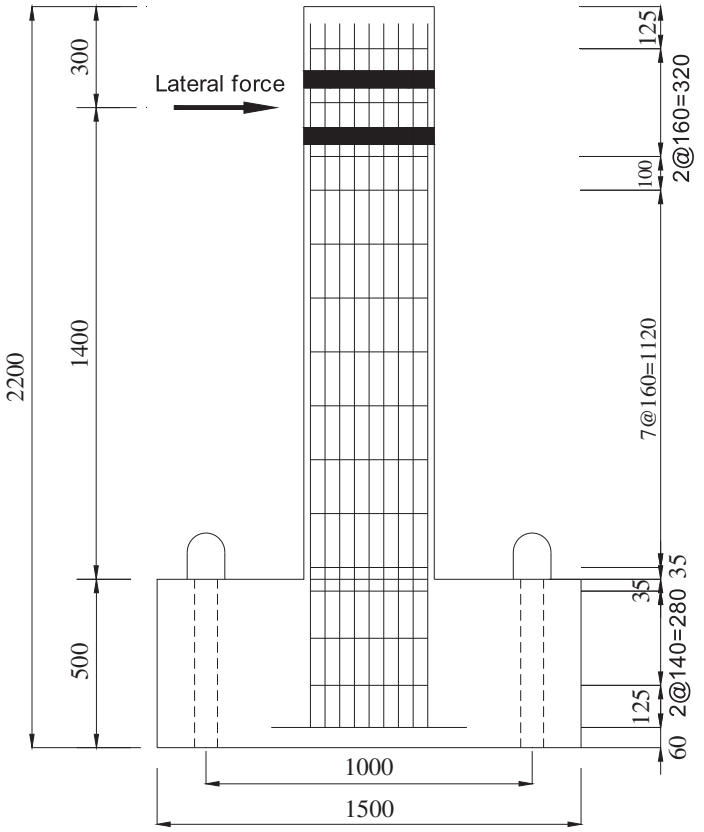

(b) General view

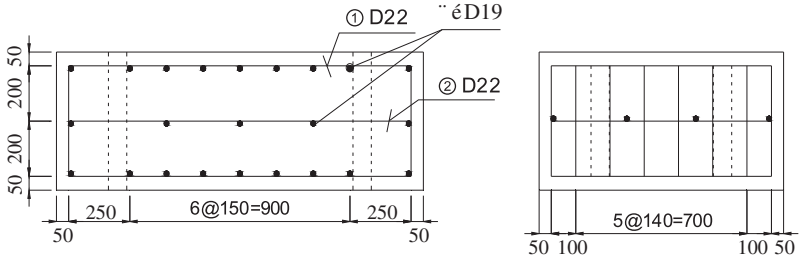

(c) Reinforcement in footing

Fig. 6. Details of the RC columns.

behavior of the continuous reinforcement specimen, but it had no effect on the flexural strength. Also, the steel jacket delayed the yield point by 11.2%.

For the lap-spliced specimen SP50-NSJ, the yield occurred at 0.618% drift ratio, which was 12.3% less than that for the SP00-NSJ specimen. Also, the drift ratio was 1.975% for the ultimate state; thus, the displacement ductility was 3.193, which was almost half of the ductility of the SP00-NSJ. When a steel jacket was applied to the lap-spliced column (SP50-SJ1), the yield and ultimate points developed at 0.665% and 5.598% drift ratios, respectively, and the

Table 2
Description of RC column specimens.

Specimen	Diameter/height (mm)	Longitudinal reinforcement		Transverse reinforcement		Steel jacket
		No. of bars/volumetric steel ratio	Lap splice (%)	Volumetric confinement steel ratio	Space (mm)	
SP00-NSJ	D=400	#16-D13	0	$\rho_s = 0.46\%$	160	Non
SP00-SJ1	H=1400	$\rho_s = 1.61\%$	0			1 mm
SP50-NSJ			50			Non
SP50-SJ1			50			1 mm

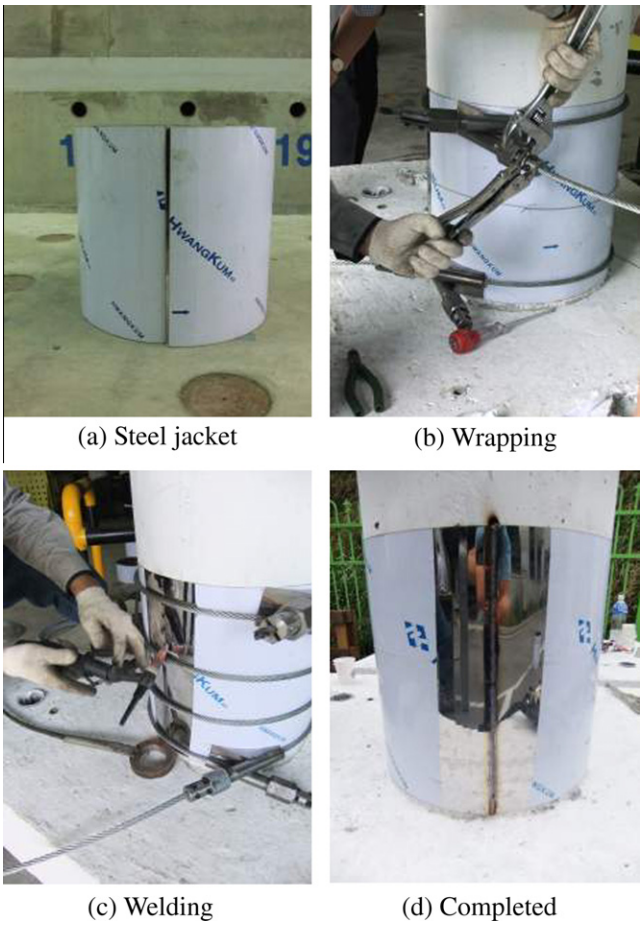

Fig. 7. Jacketing process for a column.

Fig. 8. Test set-up and instrumentation.

displacement ductility was 8.40. Thus, the steel jacket increased the ultimate drift 2.83 times. Also, the jacket increased the flexural strength by 19.4% from 79.7 kN to 95.2 kN. The strength of the jacketed lap-spliced specimen was almost identical to that of the continuous reinforcement specimens. The lap-spliced specimen was observed that the steel jacket increased the ultimate drift and flexural strength.

The initial stiffnesses of the force-deformation curves in Fig. 10 are summarized in Table 3. The jacketed specimen with the continuous reinforcements demonstrated less stiffness; however, the jacketed lap-spliced specimen demonstrated more stiffness. Therefore, it appears that the jacket did not influence the initial flexural stiffness of the columns; the steel wrapping jacket did not behave compositely with the concrete and did not influence the flexural stiffness. This non-composite behavior is beneficial in the seismic retrofitting of RC columns because it does not alter the original stiffness of the columns. The conventional steel jacketing method produces composite behaviors between the jacket and the concrete as a result of the bond of the grout so that it increases the stiffness and shortens the fundamental natural periods of the retrofitted structures. The increased stiffness may draw more seismic acceleration into the columns; thus, the effectiveness of the steel jackets could be reduced.

4.2. Failure modes

Fig. 11 shows the failure mode of each specimen. The continuous reinforcement specimen SP00-NSJ demonstrated a typical buckling failure of reinforcement. The reinforcing bars located furthest from the neutral axis were buckled and subsequently fractured. The specimen demonstrated yielding behavior because of the yield of reinforcement, and the cover concrete was spalled off. The reinforcement was not protected from the buckling as a result of the spalling of concrete cover, and the flexural strength was degraded in relation to the buckling of the reinforcement. For the jacketed continuous reinforcement specimen SP00-SJ1, the buckling of the reinforcing bars was delayed since the cracked cover concrete was confined by the jacket, which postponed the reinforcing bars from the buckling. Accordingly, the flexural strength of the specimen was maintained after the yield until the drift ratio of 6.44% was reached. The abrupt degradation of the flexural strength in Fig. 9b was caused by the tensile fracturing of the reinforcing bars. The reinforcing bars in Fig. 11b were bent much less than those in Fig. 11a.

For the lap-spliced specimen SP50-NSJ, the flexural strength was 21.8% lower than that of specimen SP00-NSJ because the

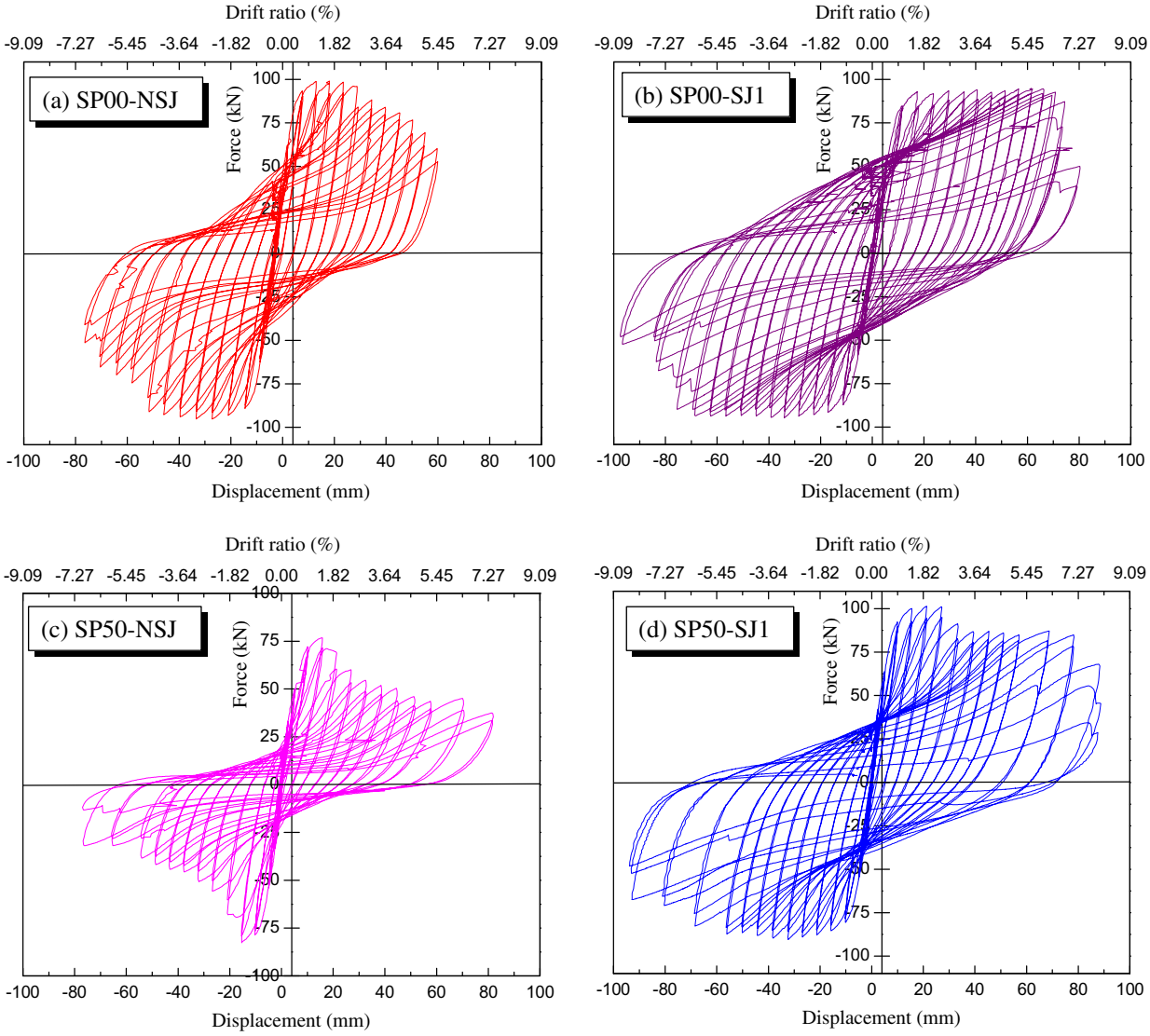

Fig. 9. Force–displacement hysteretic curves.

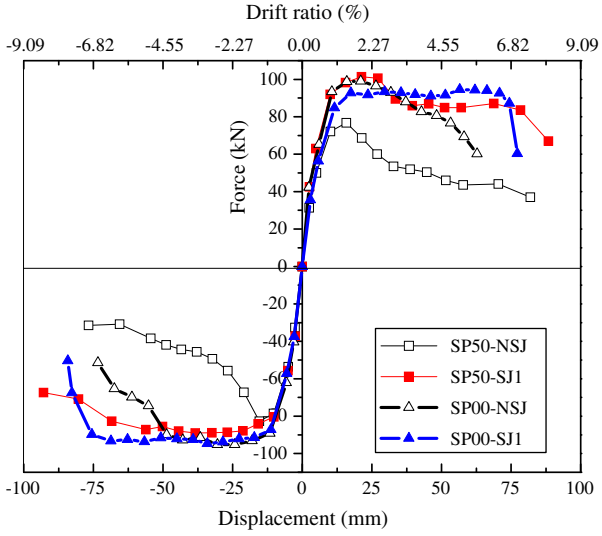

Fig. 10. Envelopes of force–displacement curves.

lap-spliced reinforcements failed due to slippage before yielding. After the failure, the flexural strength degraded sharply. The continuous reinforcements in the specimen were buckled and lost strength continuously. When the lap-spliced specimen was confined using the steel wrapping jacket, the bond strength increased and caused the lap-spliced reinforcements to yield, which increased the flexural strength to the same level as that of the continuous reinforcement specimen. Also, the jacket constrained the cracked cover concrete and delayed the buckling of the reinforcement as in the case of specimen SP00-SJ1.

5. Analysis of the bond stresses in the lap splices

Strain gauges were mounted on the surfaces of the starter bars and longitudinal bars of the as-built and jacketed columns at the plastic zones. The stresses in the bars at the measuring locations can be estimated using the measured strains and elastic-perfectly plastic behavior of steel. Using the equilibrium condition, the average bond stress (τ_b) along the surface of the starter bar can be calculated from the estimated stress of the bar as follows:

$$\tau_b = \frac{f_s d_{lb}}{4L_s} \tag{7}$$

Table 3
Summary of force–lateral displacement behavior of columns.

Specimen	Loading direction	Strength (kN)	Yield drift ratio (%)	Ultimate drift ratio (%)	Displacement ductility	Stiffness (kN/mm)
SP00-NSJ	Pushing	99.0	0.686	4.020	5.466	17.30
	Pulling	95.2	0.702	4.768	6.791	13.46
	Average	97.1	0.694	4.394	6.129	15.38
SP00-SJ1	Pushing	94.5	0.798	6.828	8.561	12.23
	Pulling	94.7	0.747	7.136	9.556	13.29
	Average	94.6	0.772	6.982	9.059	12.76
SP50-NSJ	Pushing	76.7	0.620	2.146	3.462	12.77
	Pulling	82.7	0.617	1.804	2.924	12.38
	Average	79.7	0.618	1.975	3.193	12.58
SP50-SJ1	Pushing	101.4	0.656	4.324	6.572	14.83
	Pulling	89.0	0.672	6.874	10.228	16.63
	Average	95.2	0.665	5.599	8.400	15.73

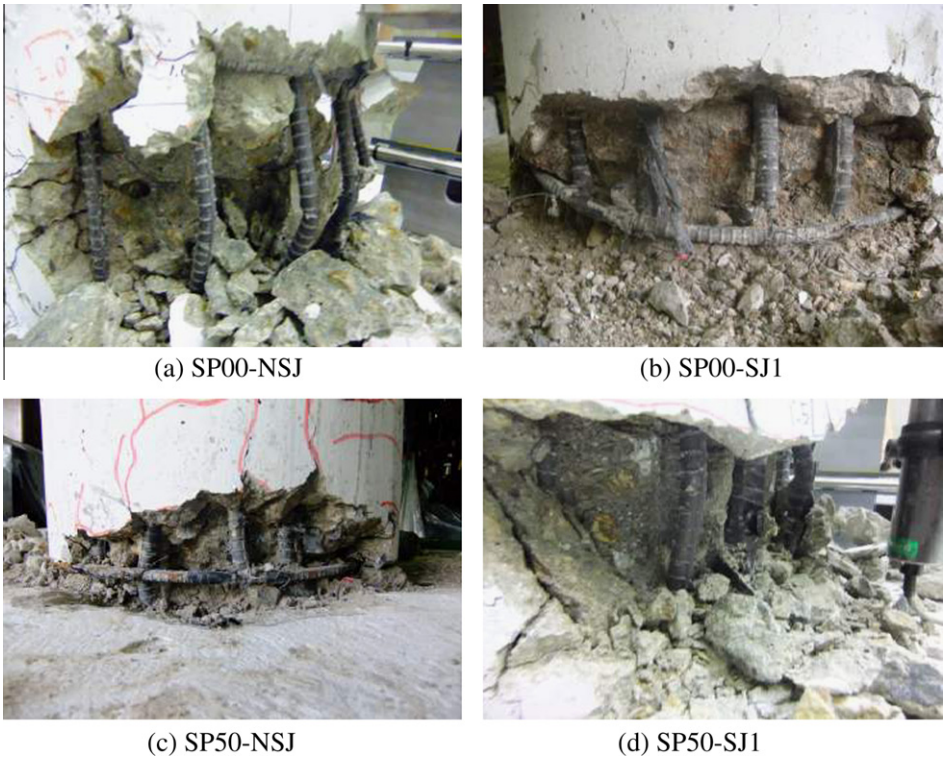

Fig. 11. Failure modes of RC columns.

where f_s is the stress at the bar; d_{lb} is the diameter of a longitudinal bar; and L_s is the length of the lap splice. Fig. 12a compares the developed stresses in the starter bars of the lap-spliced columns with the stresses in the longitudinal bars of the continuous reinforcement columns as a function of the drift ratio. When the lap-spliced column was retrofitted by the steel wrapping jacket, the developed stress in the starter bar reached the yield stress of steel (400 MPa), and it was 51% larger than the peak stress in the starter bar of the unjacketed column. Also, the starter bar demonstrated a similar trend for the stress in those of the longitudinal bars in the continuous reinforcement columns. Fig. 12b compares the stresses in the starter or the longitudinal bars of the lap-spliced columns, and the developed stress in the longitudinal bars was close to that in the starter bars. The peak bond stress of the jacketed column SP50-SJ1 was 6.5 MPa, which appeared with a yield stress of steel and was 51% larger than the peak bond stress 4.29 MPa in the unjacketed column SP50-NSJ. For the unjacketed column, the bond stress was suddenly degraded at a drift ratio of 1.78%, which corresponds to that for the peak flexural strength in Fig. 9c. For the jacketed column, the peak bond stress was developed at a drift ratio of 2.08% and was maintained at the peak value. This coincided with the behavior of the envelope curve for the column; the envelope reached the peak flexural strength at a 1.91% drift ratio and was maintained until a 3.18% drift ratio. Thus, it was found that the peak bond stress was developed at the peak flexural strength and retained until the degradation of the flexural strength.

For the continuous reinforcement columns, the steel wrapping jacket did not increase the stresses in the longitudinal bars. However, the jacket maintained the peak flexural strength up to 8.27% drift ratio without degradation, which was 2.16 times as large as the unjacketed continuous reinforcement column SP00-NSJ in Fig. 12. The more ductile behavior of the jacketed continuous reinforcement column SP00-SJ1 was resulted from the jacket delaying the buckling of the longitudinal reinforcing bars, and the delayed degradation of the flexural strength of the SP00-SJ1 was not related to the bond stress.

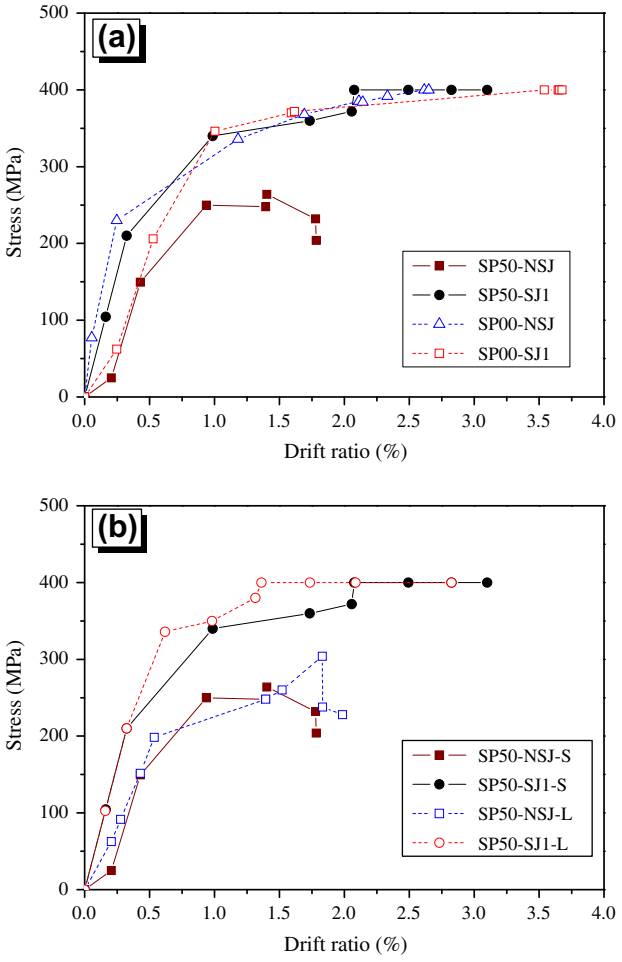

Fig. 12. Stressed developed at the starter and longitudinal bars; (a) bar-stress for unjacketed and jacketed columns and (b) stresses of the starter or the longitudinal bars in lap-spliced columns.

6. Discussion of the results and applicability

The primary roles of the steel wrapping jacket are to increase bond strength and delay the buckling of the longitudinal bars because it provides confining pressure for the lap-spliced RC columns. Therefore, the jackets increased the flexural strength and ultimate drift. For a continuous reinforcement column, the jacket did not contribute to the increase in the flexural strength because the flexural strength depended on the slip and yield of reinforcing bars. Based on the above findings, the thickness of the steel wrapping jacket should be determined from the bonding and confining actions. However, Eqs. (3)–(5), which are used to determine the thickness of the steel jacket, were based on the failure of steel during an axial compressive test as indicated by Priestly et al. [8]. The peak strength of the concrete in a compressive test was increased with a thicker steel jacket; however, the thicker steel jacket of 1.5 mm used in this study did not significantly increase the bond strength when compared with the 1.0 mm jacket. Accordingly, it appears that the thickness of the jacket has a limited ability to increase the bond strength.

Seible et al. [34] indicated that the lap splice debonding or relative slippage started at the dilation strain levels between 0.001 and 0.002. This implies that the circumferential strain of the external jacket should be less than 0.001 in order to prevent the bond slippage. Accordingly, the thickness of the jacket required for a circular column can be estimated by

$$t_j = \frac{500D(f_l - f_h)}{E_j} \tag{8}$$

where f_h represents the confining pressure provided by the transverse steel reinforcement at the strain level of 0.1%, D is the diameter of the column, and E_j is the elastic modulus of the jacket. Seible et al. [34] also suggested that the required lateral clamping pressure that can prevent the occurrence of the lap splice debonding or the relative slippage of longitudinal bars can be calculated by

$$f_l = \frac{A_{bl} f_{yl}}{[p/(2n) + 2(d_{lb} + c)]L_s} \tag{9}$$

where p is the perimeter in the column cross section along the lap-spliced bar locations, n is the number of spliced bars along p, A_{bl} is the area of one main column reinforcing bar, f_{yl} and d_{lb} are the yield strength and diameter of longitudinal bars, respectively, L_s is the length of the lap splice, and c is the thickness of the concrete cover for the longitudinal steel bars. The elastic modulus of steel is 200 GPa, and the yield strength of the steel reinforcement is 400 MPa. Thus, the f_h and f_l for the column in this study are equal to 0.578 and 1.554 MPa, respectively. If only the slippage is considered, the required thickness of the steel jacket was 0.976 mm. However, the jacket thickness required to restrain the buckling of the longitudinal reinforcement up to a demand-ductility has not yet been discussed clearly. Therefore, further study is required in order to set up a design procedure for steel jackets based on the slippage at the lap-spliced zone and the buckling of the longitudinal reinforcement.

The steel wrapping jacket was installed using the same mechanism of the prefabricated FRP sheet jacket [35], which uses a prefabricated FRP sheet for a specific column and an adhesive to attach it to a concrete surface. Steel wrapping jackets have advantages from both conventional steel and FRP jackets; the jacketing method wraps a steel plate around an RC column in the same manner as that used to apply an FRP jacket, although it does not require adhesive to attach the steel plate. The welding connects the steel jacket mechanically, thereby effectively eliminating opportunities for peel-off of the FRP jackets. The jacket can be installed in any column location and can be easily replaced by a new jacket. Furthermore, the jacketing method can use double or multi-layered jackets to secure large thickness as required, which is also a feature of FRP jackets.

The total thickness of the wrapping steel jacket will increase for an unretrofitted column with large diameter. In the case, the weight of the jacket and pressing method could be potential problems. However, to satisfy the required thickness of the jacket, a multi-layered jacket consisting of several thin plates can be provided. In addition, each layer can be comprised of two or three pieces which can be welded together in site. Thus, the proposed jacketing method of wrapping steel plates can overcome potential problems encountered during construction.

7. Conclusions

This study conducted bond strength tests of concrete confined by steel wrapping jackets, as well as, bending tests for RC columns jacketed by the steel wrapping jackets. This study found that the steel wrapping jacket transferred the splitting bond failure to the pull-out bond failure and increased the bond strength of the concrete. Also, it appears that the steel jacket thickness had a limited ability to increase bond strength because the jackets of 1.0 and 1.5 mm demonstrated almost identical bond strength.

The jacket in the bending tests of the continuous reinforcing RC columns contributed to increase the ultimate drift and displacement ductility because it prevented the cracked concrete cover from spalling off and thereby delaying the longitudinal reinforcing

bars from the buckling. For the lap-spliced RC column, the jacket further increased the flexural strength because the reinforcement yielded before starting the slip at the lap splice zone due to the jacket's contribution to increasing bond strength. This study estimated the developed bond stresses at the lap-spliced zones. The bond strength of the lap-spliced bar in the jacketed column was estimated as 6.5 MPa that was 1.52 times as large as that of the lap-spliced bar in the unjacketed column. The flexural strength of the jacketed lap-spliced column was 1.32 times as large as that of the unjacketed column. Consequently, it was reasoned that the increment of the flexural strength of the lap-spliced column was due to the increment of the bond stress in the lap-spliced bars providing lateral confining pressure of the steel jacket.

The critical factors of failure for the lap-spliced and continuous reinforcement RC columns were the slip in the lap-spliced zone and buckling of the reinforcing bars. Steel wrapping jackets acted on these factors to improve the seismic performance of the RC columns. Accordingly, the thickness of the steel jacket should be determined based not on the failure of steel in the compressive test of the concrete, but on the bonding and confining actions.

Acknowledgement

This study was supported by the Basic Science Research Program through the National Research Foundation of Korea funded by the Ministry of Education, Science and Technology (Project No. 2012-0456-03).

References

[1] Buckle IG. The Northridge, California earthquake of January 17, 1994: performance of highway bridges. National Center of Earthquake Engineering Research, State University of New York at Buffalo, NY, Technical, Report NCEER-94-0008; 1994.
[2] Priestley MJN. The Whittier Narrows, California earthquake of October 1, 1987 – damage to the I-5/I-605 separator. Earthquake Spectra 1988;4(2):389–405.
[3] Lee DH, Choi E, Zi G. Evaluation of earthquake deformation and performance for RC bridge piers. Eng Struct 2005;27:1451–64.
[4] Hashimoto S, Fujino Y, Abe M. Damage analysis of Hanshin Expressway Viaducts during 1995 Kobe earthquake. II: Damage mode of single reinforced concrete piers. ASCE. J Bridge Eng 2005;10(1):54–60.
[5] Moehle JP. State of research on seismic retrofit of concrete building structures in the US. Proc US–Japan Symposium and Workshop on Seismic Retrofit of Concrete Structures – State of Research and Practice 2000, Japan, Japan Concrete Institute.
[6] Chung YS, Park CK, Lee EH. Seismic performance and damage assessment of reinforced concrete bridge piers with lap-spliced longitudinal steels. Struct Eng Mech 2004;17(1):51–68.
[7] Harajli MH. Seismic behavior of RC columns with bond-critical regions: criteria for bond strengthening using external FRP jackets. ASCE J Compos Constr 2008;12(1):69–79.
[8] Priestley MJN, Seibel F, Calvi GM. Seismic design and retrofit of bridges. New York: John Wiley & Sons, Inc.; 1996.
[9] Pantelides CP, Alameddine F, Sardo T, Imbsen R. Seismic retrofit of state street bridge on Interstate 80. ASCE J Bridge Eng 2004;9(4):333–42.
[10] Pantelides CP, Duffin JB, Reaveley LD. Seismic strengthening of reinforced-concrete multicolumn bridge piers. Earthquake Spectra 2007;23(3):635–64.
[11] Bracci JM, Reinhorn AM, Mander JB. Seismic resistance of reinforced concrete frame designed for gravity loads: performance of structural systems. ACI Struct J 1995;92(5):597–609.
[12] Han SH, Hong KN, Lee JB. An experimental study on uniaxial compressive behavior of RC circular columns laterally confined with prestressing aramid fiber strap. J Korea Conc Inst 2009;21(2):159–68.
[13] Karayannis CG, Chalioris CE, Sirkelis GM. Local retrofit of exterior RC beam–column joints using thin RC jackets – an experimental study. Earthquake Eng Struct Dyn 2008;37(5):727–46.
[14] Tsonos A-DG. Performance enhancement of R/C building columns and beam–column joints through shotcrete jacketing. Eng Struct 2010;32(3):726–40.
[15] Ghobarah A, Aziz TS, Biddah A. Rehabilitation of reinforced concrete frame connections using corrugated steel jacketing. ACI Struct J 1997;94(3):283–93.
[16] Engindeniz M, Kahn LF, Zureick AH. Repair and strengthening of reinforced concrete beam–column joints: state of the art. ACI Struct J 2005;102(2):1–14.
[17] Choi E, Nam TH, Cho SC, Chung YS, Park T. The behavior of concrete cylinders confined by shape memory alloy wires. Smart Mater Struct 2008;17(6):1–10.
[18] Choi E, Chung YS, Choi JH, Kim HT, Lee H. The confining effectiveness of NiTiNb and NiTi SMA wire jackets for concrete. Smart Mater Struct 2010;19(3):1–8.
[19] Andrawes B, Shin N, Wierschem N. Active confinement of reinforced concrete bridge columns using shape memory alloys. ASCE J Bridge Eng 2010;15(1):81–9.
[20] Kajiwara S. Characteristic features of shape memory effect and related transformation behavior in Fe-based alloy. Mater Sci Eng A 1999;273–275:67–88.
[21] Janke L, Czaderski C, Motavalli M, Ruth J. Applications of shape memory alloys in civil engineering structures – overview, limits and new ideas. Mater Struct 2005;38(5):578–92.
[22] Chai YH, Priestley MJN, Seible F. Seismic retrofit of circular bridge columns for enhanced flexural performance. ACI Struct J 1991;88(5):572–84.
[23] Chai YH, Priestly MJN. Analytical model for steel-jacketed RC circular bridge columns. ASCE J Struct Eng 1994;120(8):2358–76.
[24] Aboutaha RS, Engelhardt MD, Jirsa JO, Kreger ME. Retrofit of concrete columns with inadequate lap splices by the use of rectangular steel jackets. Earthquake Spectra 1996;12(4):693–714.
[25] Choi E, Park J, Nam T-H, Yoon S-J. A new steel jacketing method for RC columns. Mag Concrete Res 2009;61:787–96.
[26] Chung YS, Park CK, Meyer C. Residual seismic performance of reinforced concrete bridge piers after moderate earthquakes. ACI Struct J 2008;105(1):87–95.
[27] Lundgren K. Pull-out tests of steel-encased specimens subjected to reversed cyclic loading. Mater Struct 2000;33(7):450–6.
[28] Choi E, Chung YS, Park J, Cho BS. Behavior of reinforced concrete columns confined by new steel-jacketing method. ACI Struct J 2010;170(6):654–62.
[29] Ciampi V, Eligehausen R, Gertero VV, Popov EP. Analytical model for deformed-bar bond under generalized excitations. Trans IABSE colloquium on advanced mechanics of reinforced concrete 1981, Delft, Netherlands. p. 53–67.
[30] Harjli MH, Hout M, Jalkh W. Local bond stress–slip behavior of reinforcing bars embedded in plain and fiber concrete. ACI Mater J 1995;92(4):343–54.
[31] ATC-32. Improved seismic design criteria for California bridges: provisional recommendations. Redwood City, CA: Applied Technology Council; 1996.
[32] American Association of State Highway and Transportation Officials (AASHTO). AASHTO standard design specification for highway bridges, Washington, DC; 1992.
[33] Caltrans. Bridge design specification. Sacramento, CA: Division of Structures, Department of Transportation; 1985.
[34] Seible F, Priestley MJN, Hegemier GA, Innamorato D. Seismic retrofit of RC columns with continuous carbon fiber jackets. ASCE J Compos Constr 1997;1(2):52–62.
[35] Xiao Y, Ma R. Seismic retrofit of RC circular columns using prefabricated composite jacketing. ASCE J Struct Eng 1996;123(19):1357–64.